

Increased potential for energy savings through increasing the cooling capacity further in diffuse ceiling ventilation

Samira Rahnama
Peter Vilhelm Nielsen
Alireza Afshari
Niels Christian Bergsøe

Title Increased potential for energy savings through increasing the cooling capacity further in diffuse ceiling ventilation

Subtitle

Serial title

Edition 1 edition

Year 2019

Authors Samira Rahnama, Peter Vilhelm Nielsen, Alireza Afshari, Niels Christian Bergsøe

Editor

Language English

Pages

References

Danish summary

Key words

ISBN

ISSN

Price

Drawings

Photos

Cover

Printer

Publisher SBI, Statens Byggeforskningsinstitut, Aalborg Universitet,
Danish Building Research Institute, Aalborg University
A.C. Meyers Vænge 15, 2450 Copenhagen SV
E-mail sbi@sbi.aau.dk
www.sbi.dk

This publication is covered by the Danish Copyright Act

Contents

Contents	3
Preface	4
Abstrakt	5
Background	6
Objective.....	7
Dissemination.....	8
Methodology.....	9
Experimental study	9
Experimental setup	9
Experimental scenarios.....	11
Simulation study	12
CFD model	12
Simulation scenarios	13
Design chart.....	13
Results and discussion.....	16
Experimental results	16
Simulation results	20
Conclusion.....	22
Future work	22
Acknowledgement	24
Bibliography.....	25

Preface

The present report describes the main findings of the research project *Increased potential for energy savings through increasing the cooling capacity further in diffuse ceiling ventilation (Øget energibesparelspotentiale ved yderligere forøgelse af kølekapaciteten ved diffus loftsindblæsning)*. The project has been carried out at Danish Building Research Institute (SBI) in collaboration with one industrial partner, Troldekt company, Denmark and Department of Civil Engineering, Aalborg University. The project has been financially supported by ELFORSK, a research and development program administrated by the Danish Energy Association under sagsnr. 876175 and projekt nr. 349-065. The project was launched in April 2017 and completed in March 2019.

Danish Building Research Institute, Aalborg University Copenhagen
Department of Energy Performance, Indoor Environment and Sustainability
of Buildings

July 2019
Søren Aggerholm
Research Director

Abstrakt

Diffus loftsindblæsning er et luftfordelingssystem, som omfatter et plenum over et nedhængt loft og perforerede plader i dele af det nedhængte loft. De perforerede plader fungerer som indblæsningsåbninger. Det er vist, at diffus loftsindblæsning har en højere kølekapacitet end konventionelle indblæsningsystemer. Systemets kølekapacitet afhænger imidlertid af en række parametre. Dette projekt præsenterer resultater af analyser af kølekapaciteten i relation til to centrale parametre, som er fordelingen af varmekilder i rummet og forholdet mellem andelen af perforerede og ikke-perforerede plader i loftet. Vurderingerne er baseret på fuldskalaforsøg i laboratoriet og et design-diagram, som udtrykker grænserne for indblæsningsluftmængden og indblæsningsluftens temperatur. Resultaterne af eksperimenterne indikerer, at den højeste kølekapacitet opnås, når varmekilderne er jævnt fordelt i rummet, og hele loftet er dækket af perforerede plader. I en situation hvor kun dele af loftet består af perforerede plader reduceres kølekapaciteten, når varmekilderne er placeret direkte under de perforerede plader. Afhængig af indblæsningsluftmængden kan systemet have en højere kølekapacitet, når loftet er kun delvist dækket af perforerede plader.

Projektet indbefatter beregninger ved hjælp af CFD til analyse af kølekapaciteten i flere scenarier end blot de som indgik i laboratorieundersøgelserne. Beregninger pågår og de vil blive præsenteret i en senere rapport.

Background

Diffuse ceiling ventilation systems are air distribution systems in which outdoor air is supplied to the occupied room through the perforated panels installed in the ceiling. In these systems, the whole or part of the ceiling is covered by diffuse panels and outdoor air is distributed in a wide plenum between the diffuse panels and the ceiling slabs. This leads to lower air velocity and allows lower supply air temperature without having thermal discomfort compared to the conventional air distribution systems (J. Fan, 2013) (P. Jacobs, 2008). Thus, diffuse ceiling ventilation systems are able to cope with a higher cooling demand compared to the conventional ones, e.g. mixing or displacement ventilation systems. Nielsen and Jakubowska analysed and compared the cooling capacity of the diffuse ceiling inlet with five other air distribution systems (P.V. Nielsen E. J., 2009). These experimental results show the ability of diffuse ceiling to handle highest thermal loads compared to all the other systems. Several parameters influence the cooling capacity of the diffuse ceiling ventilation system. The critical design parameters has been analysed by Zhang et al. (C. Zhang T. Y., 2016). They categorize the design parameters into four groups, that is: diffuse ceiling properties, plenum design, heat sources location and room height. For instance, one important parameter is the geometry of the ventilated room. The cooling capacity is much higher in a room with a lower height. Another parameter is the design of the plenum, i.e. the space above the diffuse panels, where the air is distributed. The objective is having a uniform air distribution in the plenum. Buoyancy forces generated by heat plume from the heat sources and momentum forces generated by supply air control the airflow pattern in a ventilated space. The buoyancy force is the dominant driven force in diffuse ceiling ventilation systems, due to relatively low supply air velocity that enters the room through the diffuse panels. There are therefore, two essential parameters setting the airflow pattern in the room to consider: the distribution of heat sources in the room and the ratio of perforated to non-perforated panels in the ceiling. The cooling capacity of a diffuse ceiling ventilation system consisting of stone wool elements were tested by Nielsen et al. in a room with the dimension of 6 m length, 4.65 m width, 2.5 m height (P.V. Nielsen R. V., 2015). Experimental results obtained from testing three different heat sources distribution reveal that evenly distributed heat sources provide a higher cooling capacity than when heat sources are concentrated in one place. Diffuse ceiling ventilation system with three different ratio of perforated to non-perforated panels in the ceiling, were tested by Zhang et al. (C. Zhang M. K., 2016). Experimental results show that the system with partial coverage in the ceiling can develop a higher cooling capacity than systems with diffuse panels covering the whole ceiling. However, heat sources were exactly located below the perforated panels in the experiments with partial coverage. The distribution of heat sources, particularly in relation to diffuse perforated panels in the ceiling, is a key parameter, which needs further investigation. In this project, the dependence of the cooling capacity on the distribution of heat sources in the room and the ratio of perforated to non-perforated panels in the ceiling is assessed.

Objective

The objective of the project is to analyze the potential for energy saving through increasing the cooling capacity further using diffuse ceiling ventilation. In this project, the following research questions have been addressed:

- 1 How does the cooling capacity of the diffuse ceiling ventilation system depend on the distribution of heat sources in the occupied room?
- 2 How does the cooling capacity of the diffuse ceiling ventilation system depend on the distribution of diffuse panels in the ceiling?
- 3 How does the cooling capacity of the diffuse ceiling ventilation system depend on the relative location of the heat sources and the diffuse panels?

The project comprises a combination of CFD-calculations and laboratory investigations.

Dissemination

The outcome of this project has been disseminated through the following conference paper:

“Evaluating the cooling capacity of diffuse ceiling ventilation system – Full-scale experimental study”

Authors: Samira Rahnama, Peter Vilhelm Nielsen, Alireza Afshari, Niels Christian Bergsøe, Hicham Johra, Rasmus Lund Jensen

Presented at Clima 2019 conference, 26-29 May, Bucharest, Romania and has been accepted for publication in the proceedings of the conference in the E3S journal.

In addition, one journal paper is under preparation, in which the results regarding the CFD simulations will be presented.

The current report has been written based on the above mentioned paper.

Methodology

This research study is based on full-scale laboratory experiment as well as CFD simulation. This section describes the methodology has been used to carry out the experimental and simulation studies.

Experimental study

This section describes the laboratory experimental setup, the scenarios that were tested at the laboratory and the method that is applied in order to compare the different experimental scenarios.

Experimental setup

Figure 1 shows the outside and inside view of the so-called “Guarded Big Hot Box” test room with the internal dimension of 4.2 m length, 3.6 m width and 2.5 m height (C. Zhang P. H., 2015).



Figure 1: Outside and inside view of the test room in Aalborg University laboratory, Department of Civil Engineering

The diffuse ceiling consisted of wood fiber wool cement panels with the dimension of 0.025 x 0.6 x 1.2 m (see Figure 2). Six electric lamps attached to six cylinders with the height of 1.1 m were used as heat sources in the room.

The input electrical power to the lamps was varied through a regulator in order to have different heat loads in different experimental scenarios. Air velocity and air temperature were measured and logged with Dantec hot-sphere anemometer probes at 45 points in the test room.



Figure 2: A wood wool cement panel from Troldekt company

15 poles with three anemometers installed on each are placed in the room. The anemometers were located at the heights of 0.1 m, 1.1 m and 1.8 m on each pole according to DS/EN 15726 standard (standard D. 1., 2012) for measurements in the occupied zone for evaluation of thermal conditions. The accuracy of velocity measurement is ± 0.02 m/s for the range of 0-1 m/s (M. H. Kristensen, 2015). Figure 3 shows the placement of the poles on the floor. The poles were placed with 0.5 m distance from the walls in order to cover the occupied zone based on recommendations from DS/EN 13779 (standard D. 1., 2007).

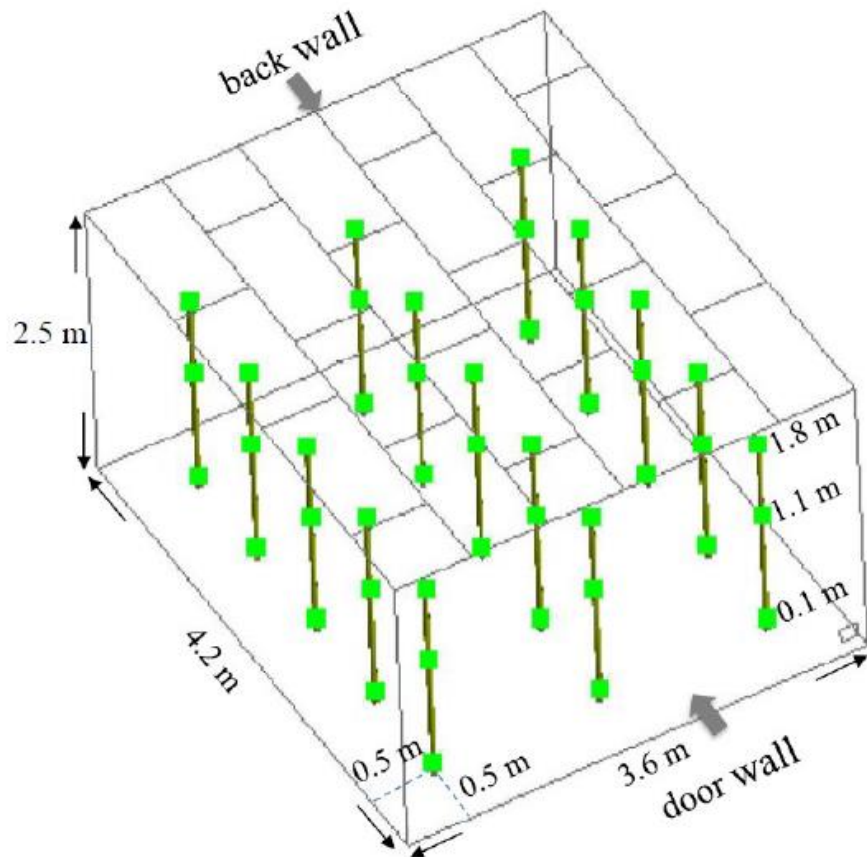


Figure 3: Location of poles on the floor and location of anemometer probes on each pole

The ventilation supply airflow rate to the room was controlled by a frequency transformer connected to the supply fan. The former was measured with an orifice plate and a pressure difference transducer. Supply and exhaust airflow rate were adjusted so that the pressure difference between the room

and the laboratory space was close to zero. Supply and exhaust air temperature were measured with type-k thermocouples placed inside the supply and exhaust air ducts and were logged with a Fluke Helios 2287 data logger. The uncertainty of the temperature instrument is ± 0.15 K (J. L. Dreau, 2014). Temperatures inside the guarded thermal zones surrounding the test room were measured in several locations.

Experimental scenarios

Four scenarios, illustrated in Figure 4, with different distribution of heat sources and ratios of perforated to non-perforated panels in the ceiling were tested:

1. Scenario 1 is with 100% perforated diffuse panels and evenly distributed heat sources.
2. Scenario 2 is with 100% perforated diffuse panels and the heat sources concentrated close to the back wall.
3. Scenario 3 is with 2.4% perforated diffuse panels and the heat sources concentrated close to the back wall.
4. Scenario 4 is with 2.4% perforated diffuse panels and heat sources close to the door wall, below the perforated panel.

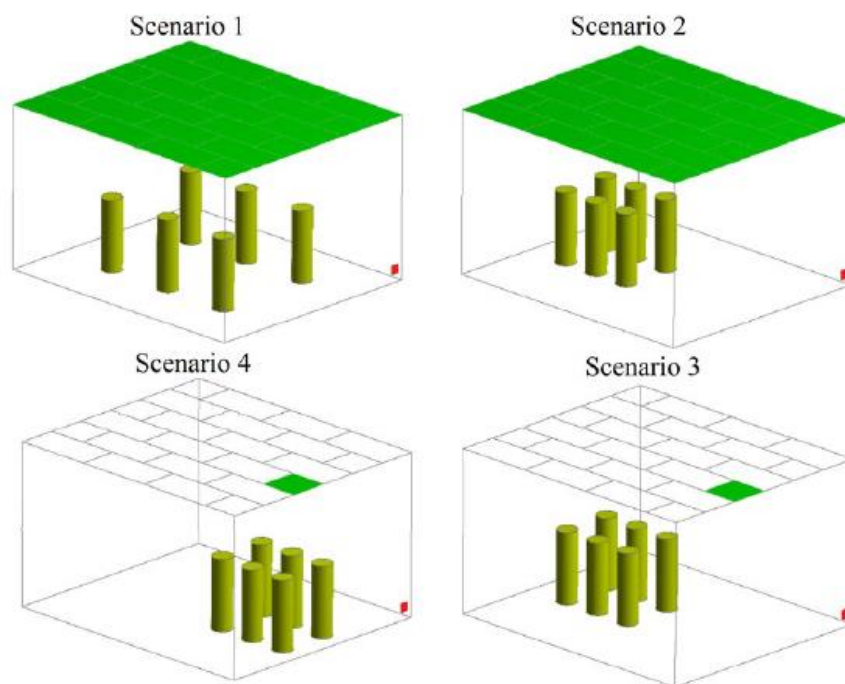


Figure 4: Four experimental scenarios with different distribution of heat sources and different ratios of perforated to non-perforated panels in the ceiling- supply and exhaust areas are highlighted in green and red on the ceiling and the door wall respectively

Two sets of experiment were conducted in Scenario 1 and Scenario 4. In one set, the heat sources were first turned on in the initial step. The ventilation system was kept off for several minutes to allow the development of buoyancy-driven airflow from the heat sources in the room. Then, the ventilation system was switched on. In the other set of experiments, the ventilation system was in operation when the heat sources were turned on, allowing the momentum-driven airflow to first develop in the room. The purpose of these experiments was to study the interaction between the two airflows and the effect of that on the airflow pattern in the room. Considering the above-mentioned scenarios, the followings have been investigated:

- The influence of heat sources distribution on the cooling capacity when the diffuse panels cover the entire ceiling (Comparison of Scenario 1 and Scenario 2)
- The influence of heat sources distribution on the cooling capacity when the diffuse panels cover part of the ceiling (Comparison of Scenario 3 and Scenario 4)
- The influence of different ratios of perforated to non-perforated panels on the cooling capacity for the same heat sources distribution (Comparison of Scenario 2 and Scenario 3)
- The influence of different initial situations, whether the ventilation system starts operation before the heat sources or vice versa

Simulation study

The diffuse ceiling ventilation system was tested experimentally in a limited number of scenarios due to practical limitations. More scenarios can be tested with CFD calculations. To this end, a CFD model was made using ANSYS Fluid Flow (Fluent) package 17.1. This section describes the CFD model.

CFD model

ANSYS DesignModeler was used to develop a 3D geometry of the room with the same dimension as the Guarded Big Hot Box. The focus of this study is on the airflow patterns in the occupied room and the airflow patterns in the plenum area is not of interest. Thus, the geometry model only consists of the room, but not the plenum to simplify the CFD model. ANSYS Meshing was used to discretize the entire room into control volumes. In order to create mesh with a higher quality, the heat sources were built as rectangular, but with the same surface area as the cylinder heat sources. The commercial CFD program Fluent was used to solve the airflow and temperature distribution in the room. The setup is as follows:

- The RNG $k-\epsilon$ turbulence model together with Enhanced Wall Treatment was used to simulate the turbulent flow in the room.
- The buoyancy-driven flow was considered with the Boussinesq approximation.
- The walls of the room, the floor area and the passive part of the ceiling were modeled as constant temperature boundary condition, where the average measured temperature obtained from the experiments were used in the CFD model.
- Heat sources were modeled with a constant heat flux boundary condition. Since the radiation is disabled in the CFD model, half of the measured heat load was used in the simulation model in order to just model the convective heat release.
- The inlet is modeled as velocity-inlet, where the measured airflow rate divided by the surface area of the active part of the ceiling was used for the velocity magnitude (Normal to Boundary).
- The outlet was modeled as outflow.
- The SIMPLE scheme with second-order upwind discretization method was employed.
- The convergence criteria were set to 10^{-4} , except for continuity 10^{-6} and energy 10^{-8} .

The CFD model should be first validated before running further simulation scenarios. The validation is based on the experimental measurements. The CFD simulation provides predicted value of the average air velocity in the

room. The predicted values are compared with the measurements at several locations and in at least two of the experimental scenarios.

Simulation scenarios

Several scenarios can be considered in the simulation study. An example is given in Figure 5, There are three scenarios which have almost 29% perforated diffuse panels in the ceiling with three different locations of heat sources (Scenario 5, Scenario 6 and Scenario 7). Scenario 8 and Scenario 9 are with 33% perforated diffuse panels. In Scenario 8, the diffuse panels spread out in the ceiling, such that they are not above the heat sources, whereas, in Scenario 9, the diffuse panels are placed above the heat sources. Scenario 10 is with 36% diffuse panels and the heat sources concentrated close to the back wall.

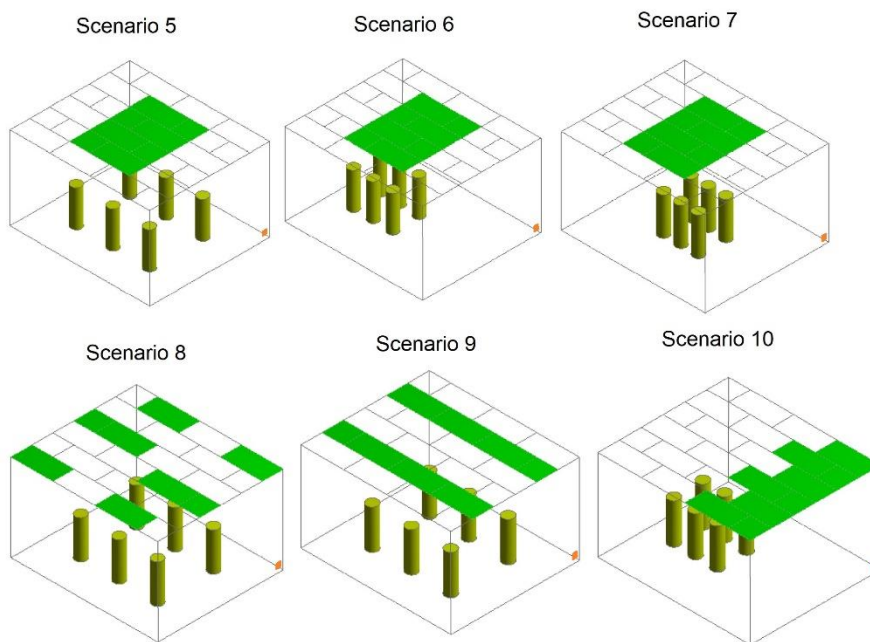


Figure 5: Simulation scenarios - supply and exhaust areas are highlighted in green and red on the ceiling and the door wall respectively

Design chart

A design chart method has been developed by Nielsen (Nielsen, 2007), which makes it possible to compare different air distribution systems in a certain situation. The design chart is a q_0 - ΔT_0 chart, where q_0 [m^3/s] is the supply airflow rate and ΔT_0 [$^{\circ}\text{C}$] is the temperature difference between the supply and exhaust air. The idea is to find the limits on the supply airflow rate, and the temperature difference of the supply and exhaust air while an acceptable comfort level is satisfied. There are upper and lower limits on q_0 and ΔT_0 due to limits on draft, room temperature gradient, indoor air quality, cooling capacity, the design of the duct system, etc. (see Figure 6)

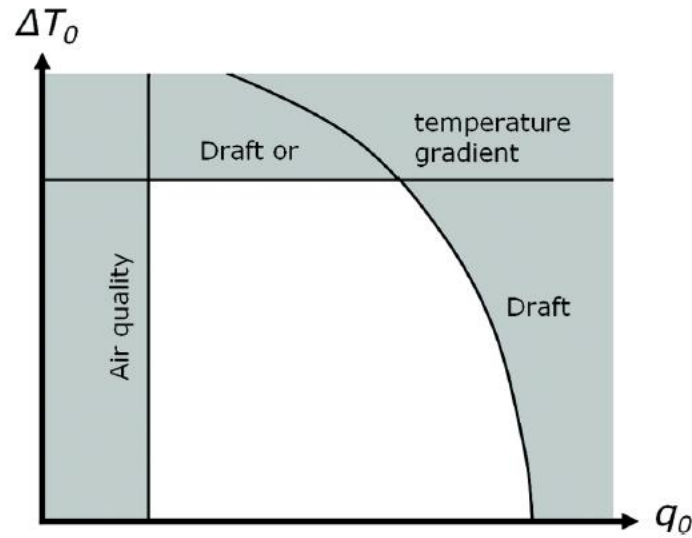


Figure 6: Design chart showing the restrictions on the flow rate q_0 and on the temperature difference ΔT_0 between return and supply owing to draft, temperature gradient, and air quality (Nielsen, 2007)

The focus in this study is on evaluating the cooling capacity of the system represented as the product of q_0 and ΔT_0 :

$$Q = \rho c_p q_0 \Delta T_0 \quad (1)$$

Where, Q [W] is the cooling capacity, i.e. the heat load that can be removed by an air distribution system, c_p [J/kg.°C] is the specific heat capacity and ρ [kg/m³] is the density of air. The objective is to compare the cooling capacity of the system in connection with the heat sources distribution in the room and the ratios of perforated diffuse panels to non-perforated panels in the ceiling. To make comparison, the cooling capacity has been calculated when the maximum air velocity in the room is limited to a certain value. The air velocity in the room is a parameter which affects the thermal comfort. The design charts can be based on any acceptable maximum air velocity. Similar to the previous works, the maximum velocity of 15 cm/s is considered in this paper.

In order to obtain points on the design chart, the laboratory experiments were conducted as follows:

- The measurements during a steady state period of three hours were used, when the supply airflow rate, supply air temperature and supply power to the heat sources were adjusted to certain values and the room temperature was stable.
- The air velocities were logged every 0.2 seconds at the locations shown in Figure 3.
- Running average velocities over 3 minutes, according to DS/EN 13182, (standard D. 1., 2002) are calculated for each anemometer probes during the three hours of the test.
- The maximum value for each measuring probe is selected, among the samples which covers the 97% of entire period. This provides 45 samples corresponding to 45 measuring probes, of which, the maximum value is considered to evaluate the air velocity in the room.

This velocity can be considered for the point with the adjusted heat load, supply airflow rate and supply air temperature. However, an additional calculation is required in order to be able to compare the different cases.

It is desired to have a fixed and known heat load during the steady-state measurement periods. In order to prevent heat flux between the test room and the surrounding environment, the room temperature should be kept equal to the surrounding guarded zone temperature. In this situation, the heat load is equal to the adjusted heat load of the heat sources. However, in practice, a temperature difference between the test room and the surrounding environment is inevitable. This has been addressed by recalculating ΔT_0 based on the measured Q and q_0 using Eq. (1), rather than using the measured ΔT_0 in obtaining the points on the design chart. The points with the recalculated ΔT_0 are the points in which the heat flow in the room is only generated by the heat sources. The momentum flow arising from the heat flow through the envelope is small compared to the momentum flow from the heat sources due to rather small temperature difference between the test room and the surrounding environment during the experiments. Thus, the influence of heat flow through the envelope on the air velocity in the room is assumed to be negligible.

The same procedure is repeated using the predicted values obtained from the CFD simulations, in order to provide the design chart for the simulation scenarios.

Results and discussion

This section provides the experimental results and the results for the validation of the CFD model.

Experimental results

The experiments were performed at three different ventilation inlet airflow rates equal to 40 l/s, 80 l/s and 100 l/s providing three points on the design chart for each scenario. In practice, it is unlikely to run experiments which yields the air velocity exactly equals to 15 cm/s. One can run several experiments and use interpolation techniques to obtain the point with a certain velocity. In this study, at least two experiments were performed at each above-mentioned airflow rate. In these experiments, either the heat load or the supply temperature were set differently. Then, linear interpolation and/or extrapolation were applied to find the points with the desired air velocity.

Figure 7 shows the design graph for Scenario 1 and Scenario 2 to see the influence of heat sources distribution in the 100% ratio of perforated to non-perforated panels in the ceiling. The points with 15 cm/s velocity are connected through straight lines to form the constant velocity curves. The results indicate the higher cooling capacity of the system in Scenario 1 compared to Scenario 2. The system with evenly distributed heat sources is able to remove a higher heat load than the system with heat sources concentrated to one corner at the same thermal condition, i.e. the air velocity of 15 cm/s and the average room air temperature equal to the surrounding environment temperature. The laboratory temperature variations were not considerable (between 21

°C to 23 °C) during the measurements in all scenarios and the laboratory temperature can be assumed constant. Similar results are obtained in (P.V. Nielsen R. V., 2015) for the same experiment, but in a larger room and with a different ceiling material.

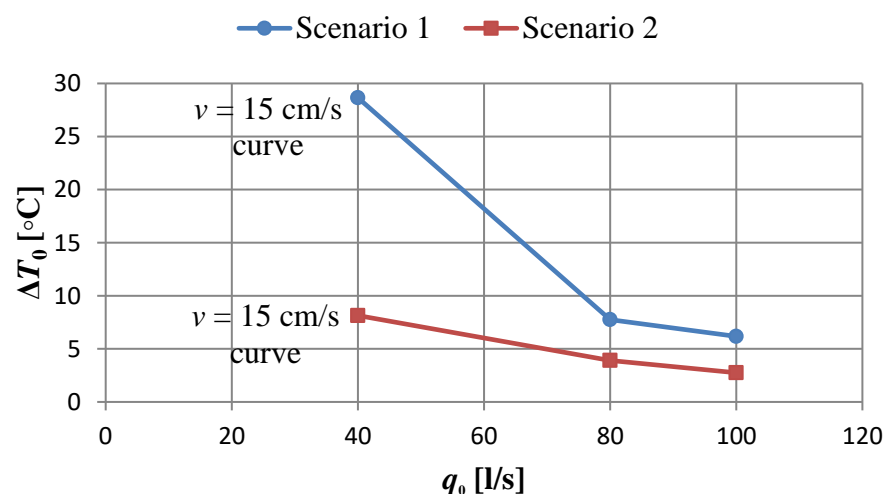


Figure 7: Design graph showing the constant velocity curves of 15cm/s for Scenario 1 (100% diffuse ceiling and evenly distributed heat sources) and Scenario 2 (100% diffuse ceiling and the heat sources concentrated close to the back wall)

Figure 8 shows the design graph for Scenario 2 and Scenario 3 to see the influence of different ratios of perforated to non-perforated panels in the ceiling in the same heat sources distribution. The constant velocity curve of 15 cm/s is shown for Scenario 2. For Scenario 3, a point with 15 cm/s is obtained at the supply airflow rate of 40 l/s. However, as the supply airflow rate increased during the experiment, the air velocity in the room increased rapidly. Practically, it was not possible to reach a point with the air velocity of 15 cm/s at the supply air flow rates higher than 40 l/s with the available experimental setup. To understand the increasing rate of air velocity in the room, the constant heat load curve of 470 W is shown for Scenario 3. The curve has a hyperbolic form which indicates the constant value for the product of q_0 and ΔT_0 representing the heat load. As shown, the air velocity is considerably higher in higher supply airflow rates in order to remove the same heat load. This translates to considerably lower cooling capacities in higher supply airflow rates for providing the same thermal comfort.

The results show that the system with 2.4% diffuse panel ratio in Scenario 3 has a higher cooling capacity than the system with 100% diffuse panel ratio at the supply airflow rate of 40 l/s. This is consistent with the earlier results obtained (C. Zhang M. K., 2016). There, the system with 18% diffuse panel is showing a higher cooling capacity than the system with 100% diffuse panel, where the heat sources were exactly located below the diffuse panels in the experiments with 18% diffuse panel. Here, the same result can be seen at the supply airflow rate of 40 l/s, even though the heat sources were located far from the diffuse panels in Scenario 3. In the small diffuse panel ratio of 2.4%, the ventilation system is similar to a mixing ventilation system and mainly momentum-driven, especially in the higher airflow rates. Thus, the curve is expected to fall down, i.e. the cooling capacity decreases to zero rapidly, similar to the mixing ventilation graph shown in (Nielsen, 2007). In fact, the areas close to the diffuse panel in Scenario 3 and Scenario 4 is outside the occupied zone, due to rather high air velocity in these areas. Thus, the air velocities measured just below the diffuse panel are not taken into account when calculating the maximum air velocity in Scenario 3 and Scenario 4.

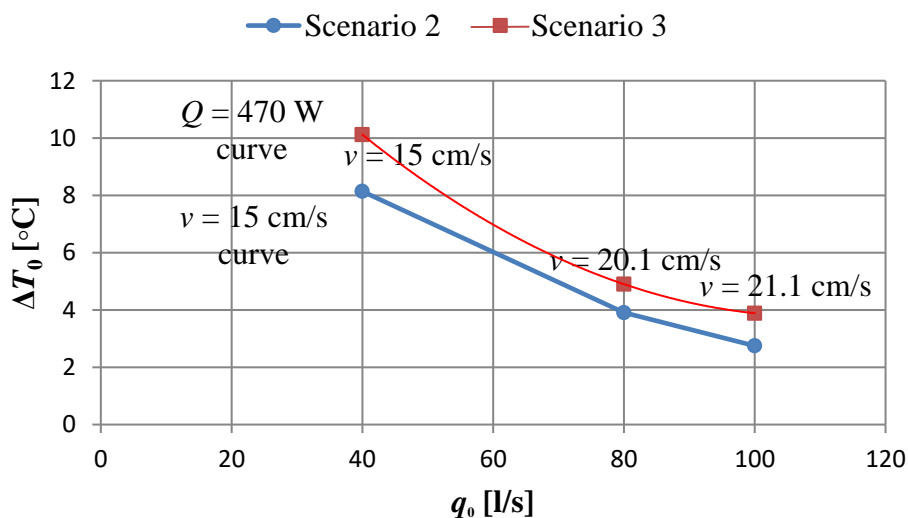


Figure 8: Design graph showing the constant velocity curve of 15cm/s for Scenario 2 (100% diffuse ceiling and the heat sources concentrated close to the back wall) and the constant heat load curve of 470W for Scenario 3 (2.4% diffuse ceiling and the heat sources concentrated close to the back wall)

Figure 9 shows the design graph for Scenario 3 and Scenario 4 to see the influence of heat sources distribution in the 2.4% ratio of diffuse panel in the ceiling. Again, due to practical limitations, it was not possible to measure the

points with the air velocity close to 15 cm/s for these scenarios. Thus, an accurate interpolation is not possible in order to provide the constant velocity curves of 15 cm/s. Instead, the constant heat load curve of 470 W is shown together with the air velocity correspond to each point for each scenario. The air velocities are higher in Scenario 4 than in Scenario 3 in order to remove the same heat load. This indicates the higher cooling capacity of the system in Scenario 3 than in Scenario 4 at the same thermal comfort condition. The cooling capacity reduces when the heat sources are placed below the diffuse panel while the major part of the ceiling is made of non-perforated panels.

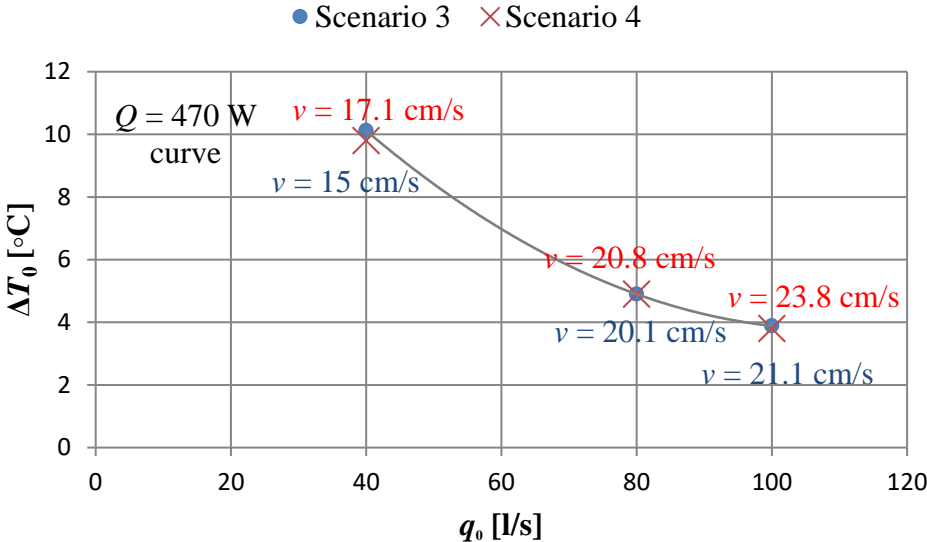


Figure 9: Design graph showing the constant heat load curves of 470 W for Scenario 3 (2.4% diffuse ceiling and the heat sources concentrated close to the back wall) and Scenario 4 (2.4% diffuse ceiling and the heat sources concentrated close to the door wall)

Figure 10 shows the design graph for Scenario 1 in the two sets of experiments explained in Experimental scenarios Section, to see the influence of different initial situations, whether the ventilation system starts operation before the heat sources or vice versa. The constant velocity curves of 15 cm/s are shown. The experimental results indicate that the influence is insignificant for the supply airflow rate of 80 l/s and 100 l/s. However, the cooling capacity is higher when the heat sources started operation first for the supply airflow rate of 40 l/s.

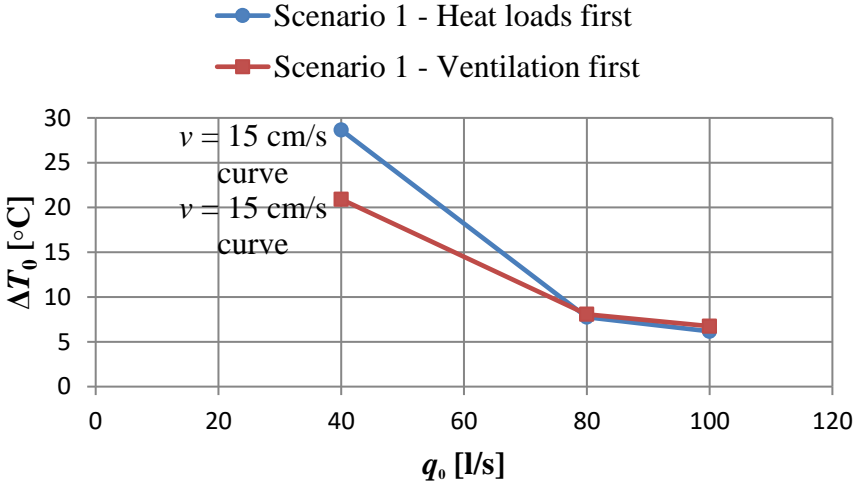


Figure 10: Design graph showing the constant velocity curves of 15 cm/s for Scenario 1 (100% diffuse ceiling and evenly distributed heat sources) in two sets of experiments, where in one heat sources and in the other ventilation system started first.

To illustrate the differences, the velocity contours for the two sets of experiment on the surfaces 0.1 m above the floor are shown in Figure 11. The contour plots are made based on the air velocity measurements at 15 points at the supply airflow rate of 40 l/s. As can be seen, the difference between the air velocities in the entire surface is insignificant for the two experiments. The maximum air velocity occurred at the same place in both experiments, but with a difference of around 1 cm/s. This difference is insignificant and can be explained by the uncertainty of the anemometer probe measurements. Likewise, the same results were obtained for the two set of experiments tested in Scenario 4.

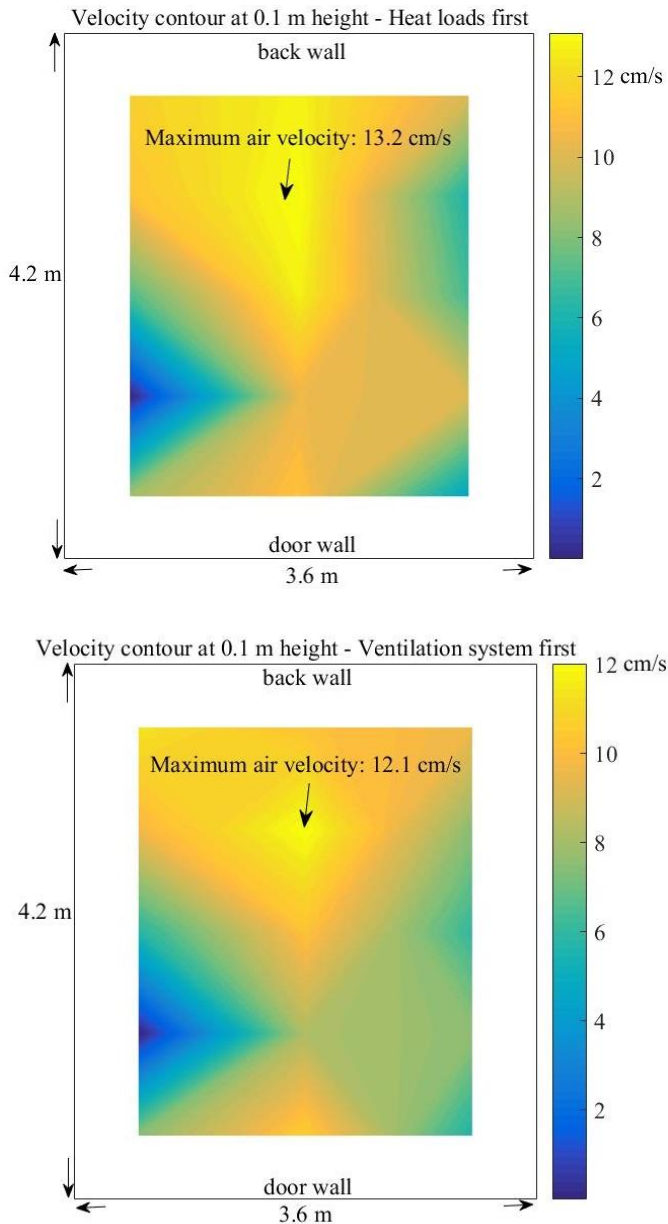


Figure 11: Air velocity contours at the surfaces 0.1 m above the floor for the experiment with heat sources started operation first (top plot) and the experiment with ventilation system started operation first (bottom plot) at the supply airflow rate of 40 l/s.

Simulation results

It should be noted that the simulation part has not been completed yet. The CFD simulation is still in progress. This section presents the simulation results for the validation of the CFD model described in CFD model Section. The results are for the pressure-based steady simulation in Scenario 1, i.e. 100% diffuse ceiling and evenly distributed heat sources. The mesh generation in CFD provides 479,496 hexahedral cells. The air velocity predicted along three lines in parallel to the three poles, pole 2, pole 8 and pole 14, are shown in Figure 12. The air velocity measurements from the anemometers installed on the poles are also shown. As can be seen, the CFD predictions are closer to the air velocity measurements at 0.1 m above the floor surface. The prediction errors are about 6%, 24% and 15% for pole 2, pole 8 and pole 14 at 0.1 m height respectively. However, the prediction error increases at the higher heights (except pole 14 at 1.1 m height) which makes the model inaccurate for this area.

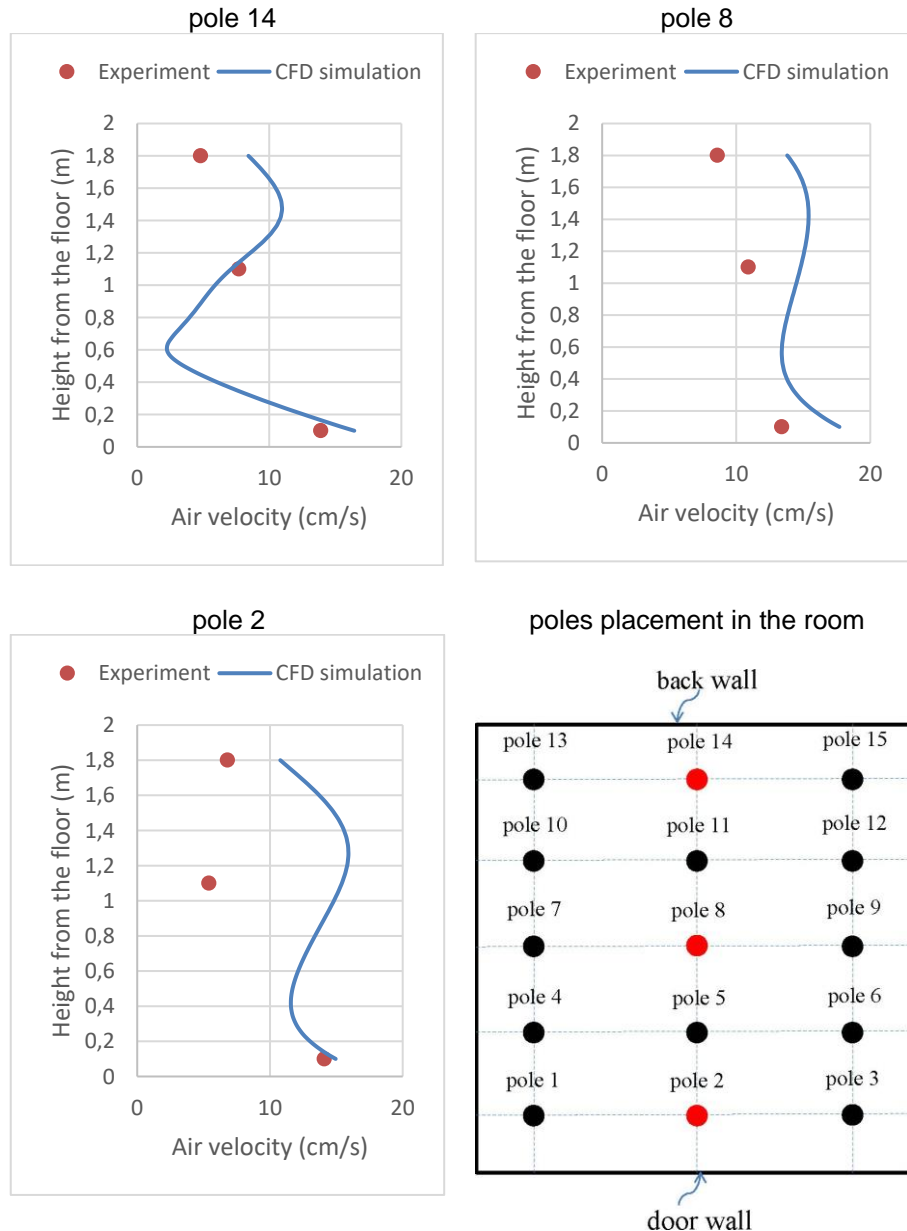


Figure 12: CFD predicted values of air velocity along three lines in the room together with the air velocity measurements at three points on each line (Scenario 1)

To better understand how the CFD model predicts the air velocity in the room, the air velocity contours on two surfaces are shown in Figure 13. Apparently, the CFD model succeeds in predicting the air velocity profile, such that the higher air velocity occurs close to the floor surface. However, the predictions are not accurate enough in the middle of the room. Thus, the CFD simulation is still ongoing at the time of writing this report. The aim is to find and simulate a CFD model which provides more accurate predictions in all area of the occupied zone with the prediction error less than 10%. Then, the next step after the model validation, will be the simulation of the scenarios presented in Simulation scenarios Section.

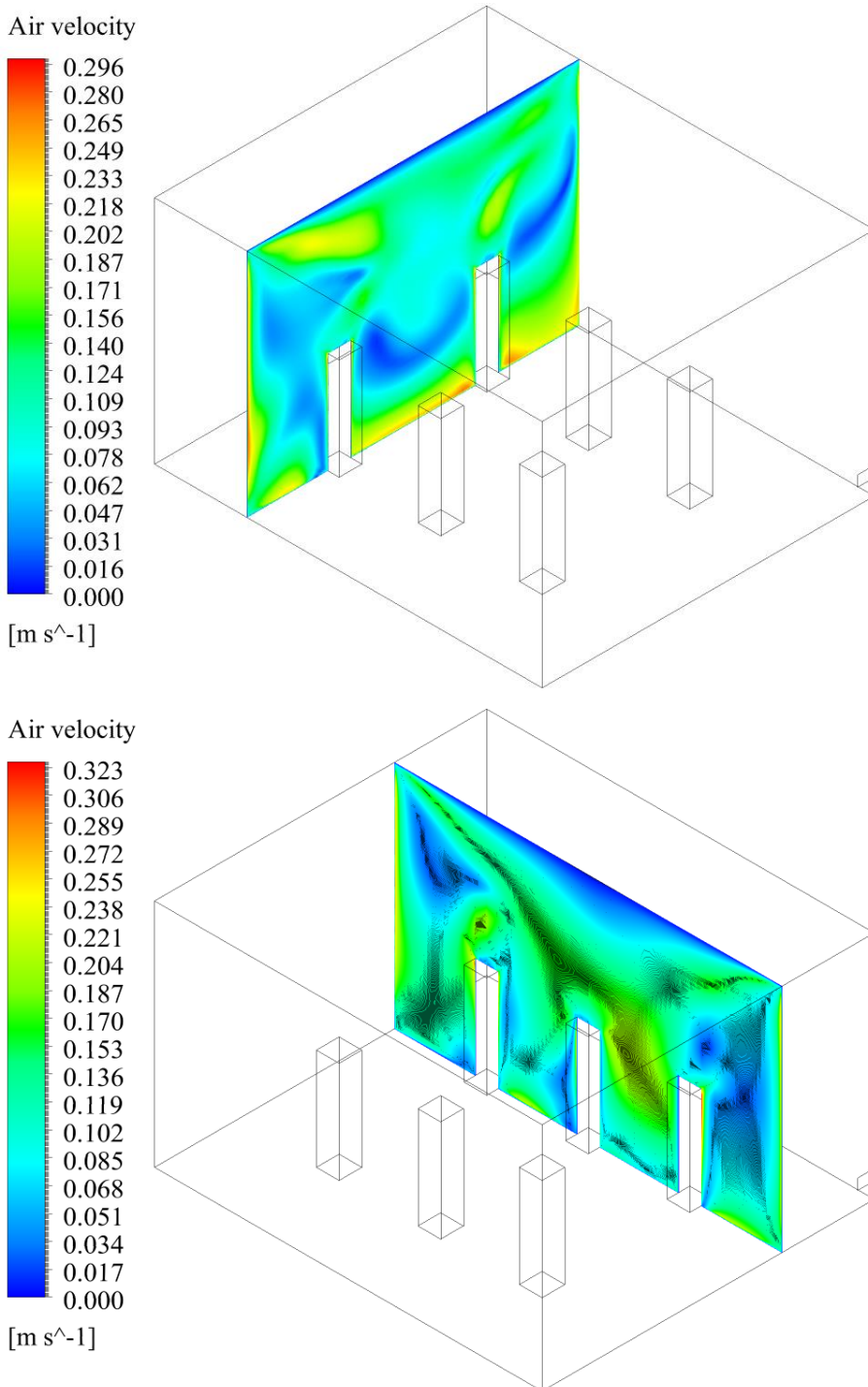


Figure 13: Air velocity contours from CFD prediction on two surfaces (Scenario 1)

Conclusion

This research evaluates experimentally the cooling capacity of the diffuse ceiling ventilation system and its dependency to the relative location of heat sources in the room and the diffuse panel area in the ceiling. Several scenarios were tested in a test room with the diffuse ceiling and the dimension of 4.2×3.6×2.5 m (L×W×H). The different scenarios were compared through a design chart showing the limits on the supply airflow rate and the temperature difference between supply and exhaust air in order to have either a constant air velocity in the room or a constant heat load removed from the room.

Two different diffuse panel ratios in the ceiling, i.e. 100% and 2.4% diffuse ceiling, were considered. In the case of 100% diffuse ceiling, the cooling capacity was higher when the heat sources were distributed evenly in the room. In the case of 2.4% diffuse ceiling, the cooling capacity reduced when the heat sources were exactly placed below the inlet diffuse ceiling. Comparing the systems with the same heat sources distribution in the two different diffuse panel ratios revealed that a higher cooling capacity is possible for a smaller diffuse panel ratio. The system with 2.4% diffuse ceiling had a higher cooling capacity compared to the 100% diffuse ceiling in the rather low supply airflow rate of 40 l/s. However, the cooling capacity reduced rapidly in the small ratio of diffuse panel with the increase of the supply airflow. In fact, the system was rather a mixing ventilation system than a diffuse ceiling ventilation system in the small ratio of perforated to non-perforated panels. In addition, several experiments were run to see the influence of different start-up operations, i.e. whether the heat sources or the ventilation starts operation first. The results showed an insignificant effect of different start-up operations on the cooling capacity.

Future work

The diffuse ceiling ventilation system was tested experimentally in a limited number of scenarios due to practical limitations. CFD simulation is required in order to investigate more scenarios. A CFD model has been made which provides acceptable predictions in area close to the floor surface of the occupied room. However, the predictions is not accurate in all area. The CFD simulation is in progress at the time of writing this report. The aim is to improve the CFD model with changing one or multiple items in the CFD model:

- Modelling the plenum area: In the current CFD model, only the occupied room is modeled. The model will maybe be improved with including a model of the plenum area. In this case, the diffuse panels will be modeled as porous media in the CFD model.
- Meshing: The grid independence check was not performed for the current CFD model. The model will maybe be improved with a higher mesh density.
- Turbulence model: The RNG $k-\epsilon$ turbulence model is used in the current CFD model, which is suggested in the literature for modeling the airflow rate in the room with diffuse ceiling air distribution system. A recent research study also suggests the SST turbulence

model when the buoyant flow is dominant. Thus, the model will maybe be improved with changing the turbulence model.

After the model validation, several scenarios will be simulated in addition to the scenarios that were tested at the laboratory:

- In 100% diffuse panels, it is shown that the cooling capacity is higher when the heat sources are distributed evenly in the room. Comparing Scenario 5 and Scenario 6 will show if this result is still valid for the partial diffuse panels in the ceiling.
- In the partial diffuse panels, it is shown that the cooling capacity reduces when the heat sources are exactly placed below the inlet diffuse ceiling. This will be further investigated with comparing the cooling capacity in Scenario 7 with Scenario 6 and Scenario 5.
- In this research as well as previous research studies, it is shown that the cooling capacity can be higher for a system with partially-covered diffuse panels than a system with 100% diffuse panels. This will be further investigated with comparing the cooling capacity in Scenario 1 with Scenario 8, Scenario 9 and Scenario 10.

Acknowledgement

The authors would like to thank Department of Civil Engineering, Aalborg University and especially, Rasmus Lund Jensen and Hicham Johra from this department who provide the possibility for full-scale experiment. In addition, the authors would like to thank Chen Zhang from this department for her support in the CFD simulation part.

This work is carried out as a collaboration between The Danish Building Research Institute at Aalborg University Copenhagen and Troldekt A/S. The project is financially supported by ELFORSK, a research and development program administrated by Danish Energy.

Bibliography

- C. Zhang, M. K. (2016). Parametrical analysis on the diffuse ceiling ventilation by experimental and numerical studies. *Energy and Building*, 111, 87-97.
- C. Zhang, P. H. (2015). Experimental study of diffuse ceiling ventilation coupled with a thermally activated building construction in an office room. *Energy and Building*, 105, 60-70.
- C. Zhang, T. Y. (2016). *Diffuse ceiling ventilation: design guide*. Department of Civil Engineering. Aalborg: Aalborg University.
- J. Fan, C. H. (2013). Performance analysis of a new design of office diffuse ceiling ventilation system. *Energy and Buildings*, 59, 73-81.
- J. L. Dreau, P. H. (2014). *Experimental data from a full-scale facility investigating radiant and convective terminals: Uncertainty and sensitivity analysis, Description of the experimental data*. Department of Civil Engineering. Aalborg University.
- M. H. Kristensen, J. S. (2015). *Air temperature measurements using Dantec Draught Probes*. Department of Civil Engineering. Aalborg: Aalborg University.
- Nielsen, P. (2007). Analysis and design of room air distribution systems. *HVAC&R Research*, 13:6, 987-997.
- P. Jacobs, E. V. (2008). Diffuse ceiling ventilation, a new concept for healthy and productive classrooms. *Indoor Air*. Copenhagen.
- P.V. Nielsen, E. J. (2009). The performance of diffuse ceiling inlet and other room air distribution systems. *Cold climate HVAC*. Sisimiut.
- P.V. Nielsen, R. V. (2015). Diffuse Ceiling Ventilation and the Influence of Room Height and Heat Load Distribution. *Healthy Building*. Eindhoven.
- standard, D. 1. (2002). *Ventilation For Buildings - Instrumentation Requirements For Air Velocity Measurements In Ventilated Spaces*.
- standard, D. 1. (2007). *Ventilation for non-residential buildings – Performance requirements for ventilation and room-conditioning systems*.
- standard, D. 1. (2012). *Ventilation for buildings – Air diffusion – Measurements in the occupied zone of air conditioned/ventilated rooms to evaluate thermal and acoustic conditions*.